

Contaminant transport with non-equilibrium processes in unsaturated soils and implicit characteristic Galerkin scheme

Xikui Li,^{1,*†} Wenhua Wu¹ and S. Cescotto²

¹*National Laboratory for Structural Analysis of Industrial Equipment, Dalian University of Technology,
Dalian 16023, People's Republic of China*

²*M.S.M. Department, University of Liege, Quai Banning 6, B-4000, Liege, Belgium*

SUMMARY

A non-equilibrium sorption—advection—diffusion model to simulate miscible pollutant transport in saturated–unsaturated soils is presented. The governing phenomena modelled in the present simulation are: convection, molecular diffusion, mechanical dispersion, sorption, immobile water effect and degradation, including both physical and chemical non-equilibrium processes. A finite element procedure, based on the characteristic Galerkin method with an implicit algorithm is developed to numerically solve the model equations. The implicit algorithm is formulated by means of a combination of both the precise and the traditional numerical integration procedures. The stability analysis of the algorithm shows that the unconditional stability of the present implicit algorithm is enhanced as compared with that of the traditional implicit numerical integration procedure. The numerical results illustrate good performance of the present algorithm in stability and accuracy, and in simulating the effects of all the mentioned phenomena governing the contaminant transport and the concentration distribution. Copyright © 2000 John Wiley & Sons, Ltd.

KEY WORDS: contaminant transport; unsaturated soil; advection–diffusion–sorption equation; characteristic Galerkin method; precise integration method; implicit algorithm

1. INTRODUCTION

The importance of the analysis of underground contaminant transport through unsaturated soils has received a great deal of attention.^{1–7} The unsaturated zone is the first zone through which contaminants penetrate before reaching aquifers, which are vital reserves of drinking water, and from which plants absorb water and nutrimental ingredients or contaminants. It is also the first zone where appropriate measures can be taken to limit or even eliminate pollutant migration in case of accidental localized spill of some harmful substance. A numerical model for predicting the solute transport of a pollutant or chemical species through the soils is indispensable to achieve a better understanding of underground contaminant transport phenomena and, moreover, to provide a tool for pollution control and water resource management.

*Correspondence to: Dr. Xikui Li, National Laboratory for Structural Analysis of Industrial Equipment, Dalian University of Technology, Dalian 16023, People's Republic of China

†E-mail: xikuili@gingko.dlut.edu.cn

Contract/grant sponsor: European Commission; Contract/grant number: CI1* CT94-0014

Contract/grant sponsor: The National Natural Science Foundation of China

The numerical model to simulate contaminant transport through unsaturated soils is composed of two coupled phases: first, the hydro-mechanical analysis of the two immiscible fluids through the porous medium in order to determine the velocity fields of water and air flows and the distribution of saturation degrees; second, the contaminant transport analysis through the porous medium. The basic concepts, the governing equations, the finite element discretization and implementation for hydro-mechanical analysis have been described in the light of the multiphase porous fluid flow approach.^{8–11} Owing to the limitation of space, the solution procedure of the moisture flow field^{9,11} will not be dealt with in this paper. The numerical modelling method presented in this paper is concerned with the second phase. It is noted that the pollutants particularly considered in the present project are nitrates and heavy metals, which are soluble in the pore water and move with the water. Hence, a numerical model of the miscible pollutant transport through unsaturated soils is developed.

Bear and Verruijt¹ described the mechanisms governing the miscible contaminant transport in a porous medium, which include advection, mechanical dispersion, molecular diffusion. In addition, three other phenomena responsible for temporary pollutant storage (or release) and inducing retardation effects, that is adsorption, degradation and immobile water effect are also considered. Biver,¹² Radu *et al.*¹³ and Xikui Li *et al.*¹⁴ integrated the above-mentioned governing phenomena into their models. The adsorption in these models is assumed to be equilibrium controlled. The models have been successfully utilized to predict many practical problems and are widely accepted for the simulation of contaminant transport through soils.

It is remarked that the influences of non-equilibrium processes on the pollutant transport in soils have been paid increasing attention. Brusseau *et al.*³ proposed a model that explicitly accounts for the effects of multiple sources of non-equilibrium involving transport—related and sorption-related processes. The immobile water effect integrated into the above-mentioned models is to consider pollutant exchange between immobile and mobile water responsible for transport-related non-equilibrium, often referred to as physical non-equilibrium. The experimental study¹⁵ on solute transport of aqueous solution with Cd^{2+} has shown that the equilibrium adsorption model cannot properly describe the real phenomena of pollutant transport of some substances such as heavy metal Cd^{2+} in soils. A non-equilibrium mechanism reflecting the chemical non-equilibrium process and arising from rate-limited interaction of the solute with specific sorption sites is integrated into the current non-equilibrium sorption–advection–diffusion model.

The difficulties in the numerical solution of advection–diffusion equations have long been recognized. It is noted that the seeping flow in porous media is usually dominated by diffusion terms, while accidental spill of some substance in pore water can yield advection dominated transport. Hence, the proper numerical methods should be utilized to solve problems with different balances of advection and sorption–diffusion terms within the same applications. It is well known that the standard Galerkin finite element method often shows oscillatory solutions, particularly in the advection dominated transport problem or if the finite element meshes are too coarse, as this method is only valid for self-adjoint equations. Many efforts have been devoted to develop stabilized methods, which may overcome instabilities and inaccuracies in the standard Galerkin method solution.^{16–19} The introduction of the characteristic Galerkin method gives great impetus to the extensive development of finite element procedures for the solution of the advection–diffusion equations. One of the main merits of the method is that it justifies the use of the Galerkin spatial discretization. In addition, the balancing diffusion term is introduced as the ‘upwinding’ in a rational form to avoid using arbitrary mesh-dependent upwind coefficients. The

success of the method in solving the sorption–advection–diffusion equation is achieved by a suitable operator splitting procedure. The key to such a split lies in a fractional step method derived originally by Chorin²⁰ for incompressible flows. Zienkiewicz *et al.*^{16,17} applied the characterized Galerkin method to the advection–diffusion problems and developed an explicit algorithm for the problems.

To take into account the retardation effects due to phenomena such as adsorption, degradation and immobile water effect, a modified version of the characteristic Galerkin method with explicit algorithm had been developed for the numerical solution of the transient advection–diffusion equation.¹⁴ The advantage of the algorithm is that it is very efficient to compute and very easy to implement while accuracy of the results obtained by the algorithm is still ensured. It is remarked that the explicit algorithm of the semi-discretized governing equation in time domain is conditionally stable and a critical time step size with rather small value, i.e. a serious limitation of the Courant number on the application of the algorithm is required to ensure the stability of the algorithm.

In view of the disadvantage of the conditional stability of the explicit algorithm, a fully implicit unconditionally stable algorithm for the non-equilibrium sorption–advection–diffusion equation is developed in the present work. The precise integration method²¹ with a 2^N algorithm^{21,22} is utilized to determine the material derivative of the convective function in the operator splitting procedure. The stability of the present integration scheme is analysed. The numerical examples demonstrate and validate the performance and the capability of the presented numerical model and the unconditional stability of the present implicit algorithm.

2. GOVERNING EQUATIONS OF NON-EQUILIBRIUM SORPTION-ADVECTION-DISPERSION MODEL

The mass balance equations for the pollutant in the mobile water, immobile water and in the solid can be given in the form

$$\frac{\partial(\theta_m c_m)}{\partial t} + \text{div}[\theta_m(c_m \dot{\mathbf{U}}_w - \mathbf{D}_h \nabla c_m)] = \theta_m \rho_w \Gamma_m + f_{im}^m - f_m^s - g_m^s + Q^* c^* \quad (1)$$

$$\frac{\partial(\theta_{im} c_{im})}{\partial t} = \theta_{im} \rho_w \Gamma_{im} - f_{im}^m - f_{im}^s - g_{im}^s \quad (2)$$

$$\frac{\partial(\theta_s \rho_s (F + F_n))}{\partial t} = \theta_s \rho_s \Gamma_s + f_m^s + f_{im}^s + g_m^s + g_{im}^s \quad (3)$$

where c_m is the pollutant volumetric concentration in mobile water, Q^* the water source flux with the concentration c^* of the pollutant species. The intrinsic phase velocity of the mobile water is given by⁹

$$\dot{\mathbf{U}}_w = \dot{\mathbf{u}} + \frac{\dot{\mathbf{w}}}{\theta_m} \approx \frac{\dot{\mathbf{w}}}{\theta_m} \quad (4)$$

with the volumetric portion held by the phase of mobile water

$$\theta_m = n(S_w - S_{w0}) \quad (5)$$

In the above, $\dot{\mathbf{w}}$ is the Darcy (average) velocity of the water and $\dot{\mathbf{u}}$ the velocity of the solid skeleton of the soil, n the porosity, S_w the saturation degree of the water, S_{w0} the portion of the immobile water in S_w , nS_{w0} the volumetric proportion held by the immobile water symbolized by

$$\theta_{im} = nS_{w0} \quad (6)$$

\mathbf{D}_h is the hydrodynamic dispersion tensor in the porous medium, which can be written as

$$\mathbf{D}_h = \mathbf{D}_m + \mathbf{D}_d \quad (7)$$

with \mathbf{D}_m the molecular diffusion tensor and \mathbf{D}_d the mechanical dispersion tensor. For an isotropic porous medium, \mathbf{D}_d is symmetric and can be expressed by¹

$$\mathbf{D}_d = a_T \|\dot{\mathbf{U}}_w\| \mathbf{I} + (a_L - a_T) \frac{\dot{\mathbf{U}}_w \dot{\mathbf{U}}_w^T}{\|\dot{\mathbf{U}}_w\|} \quad (8)$$

where \mathbf{I} is the unit matrix, a_L and a_T are the longitudinal and the transversal dispersity,

$$\mathbf{D}_m = D_m \mathbf{I} \quad (9)$$

where D_m is the molecular diffusion coefficient in the porous medium and is, in general, related to the porosity and the saturation degree.

When a linear degradation model is considered, the pollutant solute degradation per second and per unit mass for each phase can be expressed by¹³

$$\Gamma_s = -k_s F = -k_s(F_m + F_{im}) \quad (10)$$

$$\Gamma_m = -k_m \frac{c_m}{\rho_w} \quad (11)$$

$$\Gamma_{im} = -k_{im} \frac{c_{im}}{\rho_w} \quad (12)$$

where k_s , k_m and k_{im} are degradation coefficients (s^{-1}) in the solid, mobile and immobile water, respectively, ρ_w being the bulk density of water.

f_x^y is the quantity of the pollutant migrated from the phase x to the phase y per unit time in a representative element volume. For the pollutant migration between the pore fluids and the soil skeleton governed by the equilibrium sorption and the above linear degradation mechanism, it follows that

$$f_m^s = \frac{\partial}{\partial t} [(\theta_s \rho_s (1-p) K_d c_m) + k_s \theta_s \rho_s (1-p) K_d c_m] \quad (13)$$

$$f_{im}^s = \frac{\partial}{\partial t} [(\theta_s \rho_s p K_d c_{im}) + k_s \theta_s \rho_s p K_d c_{im}] \quad (14)$$

where $\theta_s = 1 - n$ is the volumetric proportion held by the solid phase and ρ_s is the bulk density of the solid phase. It is common to assume that neither hydrodynamic dispersion nor advection of a pollutant can take place in immobile water. However, there is a pollutant exchange process

between immobile and mobile water responsible for the so-called transport-related non-equilibrium. With c_{im} denoting the pollutant concentration in immobile water, the net rate of pollutant exchange, f_{im}^m , is often expressed by¹

$$f_{im}^m = \alpha_d^*(c_{im} - c_m) \quad (15)$$

where α_d^* is a first-order mass transfer coefficient from the fluid in motion to the immobile water (s^{-1}) that depends on the molecular diffusion coefficient and the geometry of the contact area between immobile and mobile water.³

The sorption mechanism is simulated by two sorption processes in the present model: the equilibrium and the non-equilibrium sorption processes. Adsorption is considered instantaneous and reversible as an equilibrium sorption process. The linear sorption isotherm law is employed to simulate the equilibrium sorption process and is extended to both mobile and immobile water. The equilibrium-sorbed solute F of pollutant species per unit mass of the solid is proportional to the concentrations of the pollutant in mobile and immobile water and is composed of two parts: one towards mobile water F_m and the other one towards immobile water F_{im} , i.e.

$$F = F_m + F_{im} = (1 - p)K_d c_m + pK_d c_{im} \quad (16)$$

where K_d is called the division or distribution coefficient (m^3/kg), p is the portion of the fluid-solid contact surface which concerns immobile fluids. In the present model, the Langmuir sorption law^{1,2,3} is utilized to simulate the non-equilibrium non-linear sorption process, in which mass change rate of pollutant is assumed to be given by

$$\frac{\partial(\theta_s \rho_s F_n)}{\partial t} = \theta_s \rho_s [K_1 \delta(F_0 - F_n)((1 - p)c_m + pc_{im}) - K_2 F_n] \quad (17)$$

where F_n is the non-equilibrium-sorbed solute of pollutant species per unit mass of the solid, K_1 , K_2 are the parameters of the non-equilibrium sorption model (generally $K_1 \gg K_2$), F_0 represents the maximum of the non-equilibrium-sorbed solute controlled by rate-limited interaction between the solute and the specific sorption sites of the sorbent, and the function $\delta(F_0 - F_n)$ is defined by

$$\delta(F_0 - F_n) = h(F_0 - F_n)(F_0 - F_n) \quad (18)$$

with the Heaviside function $h(F_0 - F_n)$. According to equations (17) and (3) we have

$$g_m^s = \theta_s \rho_s (1 - p) [K_1 \delta(F_0 - F_n) c_m - K_2 F_n] \quad (19)$$

$$g_{im}^s = \theta_s \rho_s p [K_1 \delta(F_0 - F_n) c_{im} - K_2 F_n] \quad (20)$$

It is noted that $\rho_s F$ and $\rho_s F_n$ in equation (3) can be regarded as the concentrations of the sorbed pollutant in the solid by means of equilibrium and non-equilibrium sorption processes, respectively. The terms relating to parameters K_1 and K_2 in equations (19) and (20) are responsible for the sorption and desorption processes, respectively. In contrast to the equilibrium sorption process, the non-equilibrium sorption process is irreversible if the desorption coefficient K_2 is ignored due to its small value. The sorbed pollutant rate decreases with the total amount of the sorbed pollutant F_n . It should be remarked that the equilibrium and non-equilibrium sorption

processes in the present model are assumed parallel and non-interactive for simplicity since it is assumed that the equilibrium sorption process is due to electrical (physical) attraction, i.e. intermolecular forces of attraction between molecules of the solid and adsorbed components, while the non-equilibrium sorption process is due to chemisorption, i.e. chemical interaction between the solid and the adsorbed substances. This is also the reason why we assumed the degradation in the solids in the present model occurs only in the equilibrium-sorbed components.

Substitution of equation (13), (15) and (19) into (1) gives

$$R_m \frac{\partial(\theta_m c_m)}{\partial t} + A_m(\theta_m c_m) + \dot{\mathbf{U}}_w^T \nabla(\theta_m c_m) - \text{div}(\theta_m \mathbf{D}_h \nabla c_m) - \alpha_d^* c_{im} - Q^* c^* + g_{m2}^s = 0 \quad (21)$$

where

$$A_m = \text{div} \dot{\mathbf{U}}_w + k_m + \alpha_m + \frac{\partial}{\partial t} \left[\frac{\theta_s}{\theta_m} \rho_s (1-p) K_d \right] + \frac{\theta_s}{\theta_m} \rho_s (1-p) [K_d k_s + K_1 \delta(F_0 - F_n)]$$

$$R_m = 1 + \frac{\theta_s}{\theta_m} \rho_s (1-p) K_d; \quad g_{m2}^s = -\theta_s \rho_s (1-p) K_2 F_n; \quad \alpha_m = \alpha_d^* / \theta_m \quad (22)$$

Now consider the governing equation (2) for the immobile water. Inserting equations (14), (15) and (20) into (2) we have an equation of the form

$$R_{im} \frac{\partial c_{im}}{\partial t} + A_{im} c_{im} = \alpha_{im} c_m - g_{im2}^{s*} \quad (23)$$

where

$$A_{im} = k_{im} + \alpha_{im} + \frac{1}{\theta_{im}} \frac{\partial \theta_{im}}{\partial t} + \frac{1}{\theta_{im}} \frac{\partial(\theta_s \rho_s p K_d)}{\partial t} + \frac{\theta_s}{\theta_{im}} \rho_s p [K_d k_s + K_1 \delta(F_n - F_0)]$$

$$R_{im} = 1 + \frac{\theta_s}{\theta_{im}} \rho_s p K_d; \quad g_{im2}^{s*} = -\frac{\theta_s \rho_s p K_2 F_n}{\theta_{im}}; \quad \alpha_{im} = \frac{\alpha_d^*}{\theta_{im}} \quad (24)$$

It is noted that equations (21) and (23) are no longer linear differential ones as coefficients A_m , A_{im} , g_{m2}^s , g_{im2}^{s*} etc. vary with the value of F_n and \mathbf{D}_h depends on the value of S_w within $t \in [t_n, t_{n+1}]$. Let us denote

$$H_0 = (-A_{im}/R_{im})_n; \quad H_1^t = (-A_{im}/R_{im})_t - (-A_{im}/R_{im})_n$$

$$H_1^{n+1} = (-A_{im}/R_{im})_{n+1} - (-A_{im}/R_{im})_n; \quad f_t = [(\alpha_{im} c_m - g_{im2}^{s*})/R_{im}]_t$$

$$f_{n+1} = [(\alpha_{im} c_m - g_{im2}^{s*})/R_{im}]_{n+1}; \quad f_n = [(\alpha_{im} c_m - g_{im2}^{s*})/R_{im}]_n \quad (25)$$

Substitution of notations (25) into equation (23) gives

$$\partial c_{im} / \partial t = (H_0 + H_1^t) c_{im} + f_t \quad (26)$$

We may analytically solve equation (26) approximately in the time interval for c_{im} by considering the variation of coefficients A_{im} , R_{im} and the right-hand side term of equation (26) at time

$t \in [t_n, t_{n+1}]$ as follows:

$$c_{\text{im}}^t = [\exp(H_0 \Delta t) c_{\text{im}}^n - H_0^{-1} f_n (1 - \exp(H_0 \Delta t)) - H_0^{-1} (f_t - f_n) (1 + H_0^{-1} \Delta t^{-1} (1 - \exp(H_0 \Delta t)))] / w \quad (27)$$

where $\Delta t = t - t_n$, $t \in [t_n, t_{n+1}]$ and,

$$w = 1 + H_0^{-1} H_1' [1 + H_0^{-1} \Delta t^{-1} (1 - \exp(H_0 \Delta t))] \quad (28)$$

Substitution of notations (25) into (27) gives

$$\begin{aligned} c_{\text{im}}(t) = & [c_{\text{im}}^n \exp(H_0 \Delta t) - H_0^{-1} \left[\left(\frac{\alpha_{\text{im}}}{R_{\text{im}}}_n \right) (c_{\text{m}}^{n+1} - c_{\text{m}}^n) \right. \\ & + \left[\left(\frac{\alpha_{\text{im}}}{R_{\text{im}}}_n \right) c_{\text{m}}^n + H_0^{-1} \left(\frac{\alpha_{\text{im}}}{R_{\text{im}}}_n \right) \frac{c_{\text{m}}^{n+1} - c_{\text{m}}^n}{\Delta t} \right] (1 - \exp(H_0 \Delta t))] - H_0^{-1} [c_{\text{m}}^n \Delta \left(\frac{\alpha_{\text{im}}}{R_{\text{im}}}_n \right) - \Delta \left(\frac{g_{\text{im}2}^{\text{s}*}}{R_{\text{im}}}_n \right) \\ & + \left[- \left(\frac{g_{\text{im}2}^{\text{s}*}}{R_{\text{im}}}_n \right) + H_0^{-1} \Delta t^{-1} \left[c_{\text{m}}^n \Delta \left(\frac{\alpha_{\text{im}}}{R_{\text{im}}}_n \right) + \Delta \left(\frac{g_{\text{im}2}^{\text{s}*}}{R_{\text{im}}}_n \right) \right]] (1 - \exp(H_0 \Delta t))] / w \end{aligned} \quad (29)$$

where

$$\Delta \left(\frac{\alpha_{\text{im}}}{R_{\text{im}}}_n \right) = \left(\frac{\alpha_{\text{im}}}{R_{\text{im}}}_t \right) - \left(\frac{\alpha_{\text{im}}}{R_{\text{im}}}_n \right); \quad \Delta \left(\frac{g_{\text{im}2}^{\text{s}*}}{R_{\text{im}}}_n \right) = \left(\frac{g_{\text{im}2}^{\text{s}*}}{R_{\text{im}}}_t \right) - \left(\frac{g_{\text{im}2}^{\text{s}*}}{R_{\text{im}}}_n \right) \quad (30)$$

Finally, by substituting the solution (29) for c_{im} into equation (21), we obtain the transient sorption–advection–diffusion equation with primary unknown c_{m} , governing miscible contaminant transport as follows:

$$\frac{\partial(\theta_{\text{m}} c_{\text{m}})}{\partial t} + \dot{\mathbf{U}}_{\text{w}}^{\text{T}} \nabla(\theta_{\text{m}} c_{\text{m}}) + A \theta_{\text{m}} c_{\text{m}} - \frac{1}{R_{\text{m}}} \text{div}(\theta_{\text{m}} \mathbf{D}_{\text{h}} \nabla c_{\text{m}}) + Q = 0 \quad (31)$$

where

$$A = \frac{A_{\text{m}}^*}{R_{\text{m}}}, \quad \dot{\mathbf{U}}_{\text{w}}^* = \frac{\dot{\mathbf{U}}_{\text{w}}}{R_{\text{m}}}, \quad Q = (Q_{\text{im}}(t) - Q^* c^* + g_{\text{m}2}^{\text{s}}) / R_{\text{m}}$$

$$A_{\text{m}}^* = A_{\text{m}} + \alpha_{\text{d}}^* H_0^{-1} \frac{\alpha_{\text{im}}}{R_{\text{im}} \theta_{\text{m}}} [1 + H_0^{-1} \Delta t^{-1} (1 - \exp(H_0 \Delta t))] / w$$

$$\begin{aligned} Q_{\text{im}}(t) = & - \alpha_{\text{d}}^* \left[c_{\text{im}}^n \exp(H_0 \Delta t) - H_0^{-1} \left(\frac{\alpha_{\text{im}}}{R_{\text{im}}}_n \right) c_{\text{m}}^n [-1 + (1 - H_0^{-1} \Delta t^{-1}) (1 - \exp(H_0 \Delta t))] \right. \\ & - H_0^{-1} \left[c_{\text{m}}^n \Delta \left(\frac{\alpha_{\text{im}}}{R_{\text{im}}}_n \right) + \Delta \left(\frac{g_{\text{im}2}^{\text{s}*}}{R_{\text{im}}}_n \right) \right. \\ & + \left. \left[\left(\frac{g_{\text{im}2}^{\text{s}*}}{R_{\text{im}}}_n \right) + H_0^{-1} \Delta t^{-1} \left[c_{\text{m}}^n \Delta \left(\frac{\alpha_{\text{im}}}{R_{\text{im}}}_n \right) + \Delta \left(\frac{g_{\text{im}2}^{\text{s}*}}{R_{\text{im}}}_n \right) \right] \right] (1 - \exp(H_0 \Delta t)) \right] / w \end{aligned} \quad (32)$$

To calculate the current value of the non-equilibrium-sorbed solute F_n we should solve equation (17), which can be re-written as

$$\frac{\partial S}{\partial t} = (B_0 + B_1^t)S + b_t \quad (33)$$

where

$$\begin{aligned} S &= \theta_s \rho_s F_n; \quad B_0 = -(K_1[(1-p)c_m + pc_{im}]h(F_0 - F_n) + K_2)_n \\ B_1^t &= -(K_1[(1-p)c_m + pc_{im}]h(F_0 - F_n) + K_2)_t + (K_1[(1-p)c_m + pc_{im}]h(F_0 - F_n) + K_2)_n \\ b_t &= (\theta_s \rho_s K_1 F_0 h(F_0 - F_n)[(1-p)c_m + pc_{im}])_t \end{aligned} \quad (34)$$

Similar to the solution (27) for equation (26), we can analytically solve equation (33) approximately in the time interval for F_n as follows:

$$\begin{aligned} (F_n)_t &= [\exp(B_0 \Delta t)S_n - B_0^{-1}b_n(1 - \exp(B_0 \Delta t)) \\ &\quad - B_0^{-1}(b_t - b_n)(1 + B_0^{-1}\Delta t^{-1}(1 - \exp(B_0 \Delta t)))]/w_s/(\theta_s \rho_s)_t \end{aligned} \quad (35)$$

where

$$w_s = 1 + B_0^{-1}B_1^t[1 + B_0^{-1}\Delta t^{-1}(1 - \exp(B_0 \Delta t))] \quad (36)$$

It is remarked that the pollutant concentration c_{im} in immobile water and the solute F_n sorbed onto solid skeleton of soils arising from the physical (transport-related) and the chemical (sorption-related) non-equilibrium processes, respectively, are treated as state variables at the element integration points.

3. FINITE ELEMENT DISCRETIZATION USING CHARACTERISTIC GALERKIN METHOD AND AN IMPLICIT ALGORITHM

According to the characteristic Galerkin method, we may regard \mathbf{U}_w^* as the generalized convective velocity in equation (31) and, correspondingly, the generalized convective operator can be split from the diffusive operators and written as

$$\left. \frac{d(\theta_m c_m)}{dt} \right|_{t=t_{ref}} = \left[\frac{\partial(\theta_m c_m)}{\partial t} + \mathbf{U}_w^{*T} \nabla(\theta_m c_m) \right] \Big|_{\mathbf{x}=\mathbf{x}_{ref}, t=t_{ref}} \quad (37)$$

To calculate the material derivative $d(\theta_m c_m)/dt$ in discretized form in the time domain $[t_n, t_{n+1}]$, we consider time t_{n+1} as reference time and a particular reference particle referred to as \mathbf{x}_{n+1} at the same time. We may express the particle by $(\mathbf{x}(t_{n+1}), t_{n+1})$. The same particle had its position $\mathbf{x}(t_n)$ at time t_n and may be expressed by $(\mathbf{x}(t_n), t_n)$. It is remarked that to consider the convective effect, $(\mathbf{x}(t_{n+1}), t_n)$ generally does not mean the reference particle and implies another particle, which occupied the position \mathbf{x}_{n+1} at time t_n while \mathbf{x}_{n+1} is occupied by the reference article at time t_{n+1} . For the reference particle at reference time, the discretization of the quantity

$$\left. \frac{d(\theta_m c_m)}{dt} \right|_{t=t_{ref}}$$

can be expressed by

$$\left. \frac{d(\theta_m c_m)}{dt} \right|_{t=t_{\text{ref}}} = \frac{1}{\Delta t} [(\theta_m c_m)(\mathbf{x}(t_{n+1}), t_{n+1}) - (\theta_m c_m)(\mathbf{x}(t_n), t_n)] \quad (38)$$

where $(\theta_m c_m)(\mathbf{x}(t_{n+1}), t_{n+1})$, $(\theta_m c_m)(\mathbf{x}(t_n), t_n)$ express the values of $\theta_m c_m$ of the reference particle at time t_{n+1} and t_n respectively. Denote $\phi^{n+1} = \phi(\mathbf{x}(t_{n+1}), t_{n+1})$ and $\phi_n = \phi(\mathbf{x}(t_n), t_n)$ for any function ϕ at the reference particle. It is noted that the finite element calculation does not, in general, directly provide the value ϕ_n . Instead, it provides the value $\phi^n = \phi(\mathbf{x}(t_{n+1}), t_n)$ at time t_n .

Zienkiewicz and Codina¹⁷ derived an explicit expression to calculate the value $\phi(\mathbf{x}(t_n), t_n)$ used in an explicit approximation of the characteristic Galerkin method for a typical scalar convection–diffusion problem. Based on this work, Xikui Li *et al.*¹⁴ developed a modified version of the characteristic Galerkin explicit algorithm for the solution of a sorption–convection–diffusion equation to simulate the contaminant transport problems in unsaturated–saturated soils. The algorithm is explicit and conditionally stable as the algorithm is employed to solve the discretized finite element equation in time domain. The time step size $\Delta t = t_{n+1} - t_n$ and consequently, the Courant number ($C_r = \|\dot{\mathbf{U}}_w\| \Delta t / h$, h is the typical mesh size) are limited to a rather small value by the critical time step size determined by the stability condition of the algorithm.

In the present work, an algorithm based on the precise integration procedure is developed to derive an expression to determine the value $\theta_m c_m(\mathbf{x}(t_n), t_n)$. The algorithm can also be regarded as an operator splitting procedure, in which the generalized convective operator is split from the diffusive and sorptive (self-adjoint) operators. Let us denote $\phi = \theta_m c_m$. The values $\phi^*(\mathbf{x}(t_{n+1}), t_{n+1})$ at the reference material particles, which lie on finite element mesh points \mathbf{x}_{n+1} at time t_{n+1} , are first determined under the purely generalized convective condition. The superscript $*$ for ϕ distinguishes the value of ϕ here from the real value of ϕ for the reference article \mathbf{x}_{n+1} at t_{n+1} as other mechanisms, in addition to the advection, governing contaminant transport exist.

Let us consider the solution for a typical convective equation in a time interval $\Delta t = t_{n+1} - t_n$

$$\frac{d\phi^*}{dt} = \frac{\partial \phi^*}{\partial t} + \dot{\mathbf{U}}_w^{*T} \nabla \phi^* = 0 \quad (39)$$

where $\dot{\mathbf{U}}_w^* = \dot{\mathbf{U}}_w^*(\mathbf{x}, t)$ with components \dot{U}_{wi}^* is the velocity field, which is subjected to the essential boundary conditions composed of the following two types:

$$\phi^* = \bar{\phi}, \quad \partial \phi^* / \partial t \equiv 0 \quad \text{on } \Gamma_{\phi 1}, \quad (40a)$$

$$\phi^*|_{t=0} = \bar{\phi}|_{t=0}, \quad \partial \phi^* / \partial t = \dot{\bar{\phi}}^* \quad \text{on } \Gamma_{\phi 2}. \quad (40b)$$

With the standard Galerkin finite element discretization in space

$$\phi^* = \sum \mathbf{N}_k \phi_k^* \quad (41)$$

in which ϕ_k^* is the nodal value of the function at node k . To consider the essential boundary conditions enforced, we may list all the nodal values $(\theta_m c_m)$ in a global nodal vector $\mathbf{d}^T = [\mathbf{d}_1^T \ \mathbf{d}_2^T \ \mathbf{d}_3^T]$, in which the subscripts 1, 2 and 3 stand for the free nodal variables of $(\theta_m c_m)$ and nodal variables $(\theta_m c_m)$ on $\Gamma_{\phi 1}$ and $\Gamma_{\phi 2}$, respectively. The semi-discretized form of equation (39) is obtained by the standard finite element discretization

$$\dot{\mathbf{d}}_1^* = \mathbf{H} \mathbf{d}_1^* + \bar{\mathbf{r}}_f \quad (42)$$

where

$$\begin{aligned}\mathbf{H} &= -\mathbf{M}_{11}^{-1}\mathbf{C}_{1,11}, \quad \bar{\mathbf{r}}_f = -\mathbf{M}_{11}^{-1}(\mathbf{C}_{1,12}\bar{\mathbf{d}}_2 + \mathbf{C}_{1,13}\bar{\mathbf{d}}_3 + \mathbf{M}_{13}\bar{\mathbf{d}}_3) \\ \mathbf{M} &= \int_{\Omega} \mathbf{N}\mathbf{N}^T d\Omega \quad \mathbf{C}_1 = \int_{\Omega} \mathbf{N}\dot{U}_{w,j}^* \frac{\partial \mathbf{N}^T}{\partial x_j} d\Omega\end{aligned}\quad (43)$$

Integration of equation (42) in the time interval $\Delta t = [t_n, t_{n+1}]$ with the precise integration method²¹ gives the solution

$$\mathbf{d}_1^*(\mathbf{x}_{n+1}, t_{n+1}) = \mathbf{T}\mathbf{d}_1^*(\mathbf{x}_{n+1}, t_n) + \bar{\mathbf{R}}_f = \mathbf{T}\mathbf{d}_1(\mathbf{x}_{n+1}, t_n) + \bar{\mathbf{R}}_f \quad (44)$$

where

$$\mathbf{T} = \exp(\mathbf{H}\Delta t) \quad (45)$$

$$\bar{\mathbf{R}}_f = (\mathbf{T} - \mathbf{I})\mathbf{H}^{-1}\bar{\mathbf{r}}_f \quad (46)$$

A precise method based on the 2^N algorithm for computing exponential matrices given by Zhong *et al.*²¹ and Angel *et al.*²² can be described as follows

$$\exp(\mathbf{H}\Delta t) = \left[\exp\left(\mathbf{H}\frac{\Delta t}{m}\right) \right]^m = [\exp(\mathbf{H}\delta t)]^m \quad (47)$$

where m can be chosen as an integer power of 2, i.e. $m = 2^N$. For $N = 20$, for instance, we will have $m = 1\,048\,576$. To compute the matrix $\exp(\mathbf{H}\delta t)$ with such a small value δt , we can, therefore, use the truncated Taylor expansion to approximate $\exp(\mathbf{H}\delta t)$ with sufficiently high accuracy:

$$\exp(\mathbf{H}\delta t) \approx \mathbf{I} + \mathbf{H}\delta t + (\mathbf{H}\delta t)^2/2! + (\mathbf{H}\delta t)^3/3! + (\mathbf{H}\delta t)^4/4! = \mathbf{I} + \mathbf{T}_a \quad (48)$$

It is remarked that the norm of the matrix $\mathbf{H}\delta t$ is very close to zero and, consequently, the exponent matrix $\exp(\mathbf{H}\delta t)$ is very close to the identity matrix \mathbf{I} since δt is very small in value. Hence, the entries in matrix \mathbf{T}_a are very small in value as compared with unity in the identity matrix \mathbf{I} and should be computed and stored separately during the computation of $\exp(\mathbf{H}\delta t)$ to ensure that the significant digits in \mathbf{T}_a will not be lost due to the round-off errors.

Substitution of equations (47) and (48) into (45) gives

$$\begin{aligned}\mathbf{T} &= (\mathbf{I} + \mathbf{T}_a)^{2^N} = (\mathbf{I} + \mathbf{T}_a)^{2^{N-1}} \times (\mathbf{I} + \mathbf{T}_a)^{2^{N-1}} \\ &= (\mathbf{I} + \mathbf{T}_a)^{2^{N-2}} \times (\mathbf{I} + \mathbf{T}_a)^{2^{N-2}} \times (\mathbf{I} + \mathbf{T}_a)^{2^{N-2}} \times (\mathbf{I} + \mathbf{T}_a)^{2^{N-2}} = \dots \\ &= \mathbf{I} + \mathbf{T}_a^*\end{aligned}\quad (49)$$

It is noted that

$$(\mathbf{I} + \mathbf{T}_a) \times (\mathbf{I} + \mathbf{T}_a) = \mathbf{I} + 2\mathbf{T}_a + \mathbf{T}_a \times \mathbf{T}_a \quad (50)$$

the matrix \mathbf{T} defined by equation (45) can be fulfilled by the following algorithm:

- (1) Compute \mathbf{T}_a defined by equation (48)
- (2) Perform a recursive loop over number N to compute the matrix \mathbf{T}_a^* described by the following computer pseudo language:

do $j = 1, N$

$$\mathbf{T}_a \leftarrow 2\mathbf{T}_a + \mathbf{T}_a \times \mathbf{T}_a$$

end do

$$(3) \mathbf{T}_a^* \Leftarrow \mathbf{T}_a$$

$$(4) \mathbf{T} \Leftarrow \mathbf{I} + \mathbf{T}_a^*$$

The finite element discretization of the convective equation (39) in space also gives

$$\mathbf{d}_1^*(\mathbf{x}_{n+1}, t_{n+1}) = \mathbf{d}_1(\mathbf{x}_n, t_n) \quad (51)$$

Substitution of equation (44) into equation (51) leads to

$$\mathbf{d}_1(\mathbf{x}_n, t_n) = \mathbf{d}_1^*(\mathbf{x}_{n+1}, t_{n+1}) = \mathbf{T}\mathbf{d}_1(\mathbf{x}_{n+1}, t_n) + \bar{\mathbf{R}}_f \quad (52)$$

It is remarked that the solution of the convection equation (39) by using the precise integration method is taken as a tool to obtain precise values of the function in the sense of the finite element discretization for the reference particles on the characteristic surfaces at time t_n . This will ensure the unconditional stability and accuracy of the present characteristic Galerkin method.

Now we consider the characteristic Galerkin discretization of the sorption–convection–diffusion equation (31), which is first re-written as

$$L_c = \frac{d(\theta_m c_m)}{dt} + A\theta_m c_m - \frac{1}{R_m} \text{div}(\theta_m \mathbf{D}_h \nabla c_m) + Q = 0 \quad (53)$$

The boundary conditions of equation (53) can be expressed by

(a) The essential (Dirichlet) boundary condition

$$\phi = \bar{\phi}, \quad \partial\phi/\partial t/0 \quad \text{on } \Gamma_{\phi 1} \quad (54a)$$

$$\phi|_{t=0} = \bar{\phi}|_{t=0}, \quad \partial\phi/\partial t = \dot{\bar{\phi}} \quad \text{on } \Gamma_{\phi 2} \quad (54b)$$

which should be prescribed. As the water content θ_m in the space domain and its boundary values are determined by a preceding hydro-mechanical analysis, the boundary condition for the concentration can be given according to the given boundary values of ϕ

$$c_m = \bar{c}_m \quad \text{on } \Gamma_c \quad (55)$$

(b) The natural (Neuman) boundary condition

$$-\mathbf{n}^T \mathbf{D}_h \nabla c_m = \bar{J}_n \quad \text{on } \Gamma_J \quad (56)$$

which prescribes a dispersible (diffusible) boundary condition on Γ_J , where the dispersive rate \bar{J}_n of the pollutant along the normal \mathbf{n} of the boundary has to be satisfied in a weak form. As $\bar{J}_n = 0$ is prescribed on a part of Γ_J , it implies that this part of Γ_J is undispersive. Applying the weighted residual method to the governing equation (53) along with the Neuman boundary condition (56) one can write

$$\int_{\Omega} \mathbf{W}^{*T} L_c d\Omega + \int_{\Gamma_J} \bar{\mathbf{W}}^{*T} (-\mathbf{n}^T \mathbf{D}_h \nabla c_m - \bar{J}_n) d\Gamma = 0 \quad (57)$$

where \mathbf{W}^* and $\bar{\mathbf{W}}^*$ are arbitrary weighting functions. According to the characteristic Galerkin method and equation (37), $\dot{\mathbf{U}}_w^*$ is regarded as the generalized convective velocity. For any reference particle, the first term on the left of equation (53) is discretized in the time interval Δt by

using equation (38). The discretization of the latter three terms in equation (53) can also be considered in a similar way and expressed as follows:

$$(A\theta_m c_m)_{t=t_{\text{ref}}} = \gamma(A\theta_m c_m)^{n+1} + (1 - \gamma)(A\theta_m c_m)(\mathbf{x}(t_n), t_n) \quad (58)$$

$$\frac{1}{R_m} \text{div}(\theta_m \mathbf{D}_h \nabla c_m) = \gamma \left[\frac{1}{R_m} \text{div}(\theta_m \mathbf{D}_h \nabla c_m) \right]^{n+1} + (1 - \gamma) \left[\frac{1}{R_m} \text{div}(\theta_m \mathbf{D}_h \nabla c_m) \right](\mathbf{x}(t_n), t_n) \quad (59)$$

$$Q = \gamma Q^{n+1} + (1 - \gamma)Q(\mathbf{x}(t_n), t_n) \quad (60)$$

where $\gamma \in [0, 1]$. We may take $\gamma = 0.5$ for Crank–Nicolson scheme or $\gamma = 1.0$ for backward Euler scheme.

The global unknown vector \mathbf{d}_1 and its time derivative for the reference material particle at time t_{n+1} can be expressed by

$$\mathbf{d}_1(\mathbf{x}_{n+1}, t_{n+1}) = \mathbf{d}_1^p(\mathbf{x}_{n+1}, t_{n+1}) + \gamma \Delta \dot{\mathbf{d}}_1 \Delta t \quad (61)$$

$$\dot{\mathbf{d}}_1(\mathbf{x}_{n+1}, t_{n+1}) = \dot{\mathbf{d}}_1^p(\mathbf{x}_{n+1}, t_{n+1}) + \Delta \dot{\mathbf{d}}_1 \quad (62)$$

where the predictor values of $\mathbf{d}_1^p(\mathbf{x}_{n+1}, t_{n+1})$ and $\dot{\mathbf{d}}_1^p(\mathbf{x}_{n+1}, t_{n+1})$ are defined by

$$\mathbf{d}_1^p(\mathbf{x}_{n+1}, t_{n+1}) = \mathbf{d}_1(\mathbf{x}_n, t_n) + \dot{\mathbf{d}}_1(\mathbf{x}_n, t_n) \Delta t \quad (63)$$

$$\dot{\mathbf{d}}_1^p(\mathbf{x}_{n+1}, t_{n+1}) = \dot{\mathbf{d}}_1(\mathbf{x}_n, t_n) \quad (64)$$

where

$$\mathbf{d}_1(\mathbf{x}_n, t_n) = \mathbf{T} \mathbf{d}_1(\mathbf{x}_{n+1}, t_n) + \bar{\mathbf{R}}_f \quad (65)$$

$$\dot{\mathbf{d}}_1(\mathbf{x}_n, t_n) = \mathbf{T} \dot{\mathbf{d}}_1(\mathbf{x}_{n+1}, t_n) + \dot{\bar{\mathbf{R}}}_f \quad (66)$$

$$\dot{\bar{\mathbf{R}}}_f = (\mathbf{T} - \mathbf{I}) \mathbf{H}^{-1} \dot{\mathbf{r}}_f = -(\mathbf{T} - \mathbf{I}) \mathbf{H}^{-1} \mathbf{M}_{11}^{-1} \mathbf{C}_{1,13} \dot{\mathbf{d}}_3 \quad (67)$$

It is remarked that the water seepage analysis is first carried out at each incremental time step before the pollutant transport analysis proceeds in the current algorithm. All the nodal values of the pollutant concentration can also be divided as for $\theta_m c_m$. Denote the vector \mathbf{c}_m for nodal values c_m . For clarity, the subscript 1 for the free nodal concentration vector is dropped and \mathbf{c}_m can be expressed in the form

$$\mathbf{d}_1 = \mathbf{S}_1 \mathbf{c}_m \quad (68)$$

where the diagonal matrix \mathbf{S}_1 is a sub-matrix of $\mathbf{S} = \text{diag}(\theta_{m1}, \theta_{m2}, \dots, \theta_{mn})$, in which n is the total number of nodes of the finite element mesh. With this expression, we have

$$\mathbf{c}_m(\mathbf{x}_{n+1}, t_{n+1}) = \mathbf{c}_m^p(\mathbf{x}_{n+1}, t_{n+1}) + \gamma \Delta \dot{\mathbf{c}}_m \Delta t \quad (69)$$

where

$$\mathbf{c}_m^p(\mathbf{x}_{n+1}, t_{n+1}) = \mathbf{S}^{-1}(\mathbf{x}_{n+1}, t_{n+1}) [\mathbf{d}_1(\mathbf{x}_n, t_n) + \dot{\mathbf{d}}_1(\mathbf{x}_n, t_n) \Delta t] \quad (70)$$

$$\Delta \dot{\mathbf{c}}_m = \mathbf{S}^{-1}(\mathbf{x}_{n+1}, t_{n+1}) \Delta \dot{\mathbf{d}}_1 = (\mathbf{S}^{n+1})^{-1} \Delta \dot{\mathbf{d}}_1 \quad (71)$$

The discretization in space for $(\theta_m c_m)$ and c_m in equation (53) is carried out by the standard Galerkin method as the equation is derived from a self-adjoint problem along the characteristic

and as the spatial discretization by Galerkin method is optimal. With the finite element interpolation approximation, we have

$$(\theta_m c_m) = \sum N_j (\theta_m c_m)_j \quad c_m = \sum N_j (c_m)_j \quad (72)$$

where $(*)_j$ is the value of function $*$ at nodal point j and N_j is the shape function at nodal point j for the interpolation of the function $*$ within the element. Applying the Green's theorem to the dispersive terms in the governing equation (53) and limiting the choice of the weighting functions so that

$$\mathbf{W}^* = \mathbf{N} \quad \text{on } \Omega; \quad \mathbf{W}^* = \mathbf{0} \quad \text{on } \Gamma_c; \quad \bar{\mathbf{W}}^* = -\frac{\theta_m}{R_m} \mathbf{N} \quad \text{on } \Gamma_f \quad (73)$$

We can give the finite element equation for the implicit algorithm with backward Euler scheme, that is

$$\begin{aligned} & [\mathbf{M}_{11} + \mathbf{K}_{11}^{n+1} (\mathbf{S}_1^{n+1})^{-1} \Delta t + \mathbf{C}_{2,11}^{n+1} \Delta t] \Delta \dot{\mathbf{d}}_1 \\ &= - \left[\mathbf{f}^{n+1} + \mathbf{K}_{12}^{n+1} \bar{\mathbf{c}}_{m,2}^{n+1} + \mathbf{K}_{13}^{n+1} \bar{\mathbf{c}}_{m,3}^{n+1} + \mathbf{C}_{2,12}^{n+1} \bar{\mathbf{d}}_2^{n+1} + \mathbf{C}_{2,13}^{n+1} \bar{\mathbf{d}}_3^{n+1} + \mathbf{M}_{13} \bar{\mathbf{d}}_3^{n+1} + \mathbf{M}_{11} (\mathbf{T}(\dot{\mathbf{d}}_1^{n+1})^p + \dot{\bar{\mathbf{R}}}_f) \right. \\ & \quad - \int_{\Gamma-\Gamma_f} \mathbf{N}^T \frac{\theta_m}{R_m} \mathbf{n}^T \mathbf{D}_h \nabla c_m \, d\Gamma + \int_{\Gamma_f} \mathbf{N}^T \frac{\theta_m}{R_m} \bar{J}_n \, d\Gamma + \mathbf{K}_{11}^{n+1} (\mathbf{S}^{n+1})^{-1} (\mathbf{T}(\mathbf{d}_1)^n \\ & \quad \left. + \bar{\mathbf{R}}_f + (\mathbf{T}(\dot{\mathbf{d}}_1^{n+1})^p \Delta t) + \mathbf{C}_{2,11}^{n+1} (\mathbf{T}(\mathbf{d}_1)^n + \bar{\mathbf{R}}_f + \mathbf{T}(\dot{\mathbf{d}}_1^{n+1})^p \Delta t) \right] \quad (74) \end{aligned}$$

where \mathbf{N} is the matrix of the global shape functions assembled from the shape functions of each element,

$$\begin{aligned} (\mathbf{d}_1)^n &= \mathbf{d}_1(\mathbf{x}_{n+1}, t_n); \quad \bar{\mathbf{R}}_f = (\mathbf{T} - \mathbf{I}) \mathbf{H}^{-1} \bar{\mathbf{r}}_f; \quad \bar{\mathbf{r}}_f = -\mathbf{M}_{11}^{-1} (\mathbf{C}_{1,12} \bar{\mathbf{d}}_2 + \mathbf{C}_{1,13} \bar{\mathbf{d}}_3 + \mathbf{M}_{13} \bar{\mathbf{d}}_3) \\ \dot{\bar{\mathbf{R}}}_f(\mathbf{x}_{n+1}, t_n) &= (\mathbf{T} - \mathbf{I}) \mathbf{H}^{-1} \dot{\bar{\mathbf{r}}}_f = -(\mathbf{T} - \mathbf{I}) \mathbf{H}^{-1} \mathbf{M}_{11}^{-1} \mathbf{C}_{1,13} \bar{\mathbf{d}}_3(\mathbf{x}_{n+1}, t_n) \\ \mathbf{K} &= \int_{\Omega} \frac{1}{R_m} \frac{\partial \mathbf{N}^T}{\partial x_k} \theta_m \mathbf{D}_{h,kl} \frac{\partial \mathbf{N}}{\partial x_l} \, d\Omega; \quad \mathbf{f}^{n+1} = \int_{\Omega} \mathbf{N}^T \mathbf{Q}^{n+1} \, d\Omega \\ \mathbf{C}_2 &= \int_{\Omega} \mathbf{N}^T \mathbf{A} \mathbf{N} \, d\Omega; \quad \mathbf{C}_1 = \int_{\Omega} \mathbf{N} \dot{U}_{w,j}^* \frac{\partial \mathbf{N}^T}{\partial x_j} \, d\Omega \quad (75) \end{aligned}$$

This is the form of the implicit characteristic Galerkin method for the non-equilibrium sorption–advection–diffusion equation (31) governing the contaminant transport in unsaturated soils. In equations (74) and (75), the superscript $n+1$ for matrices \mathbf{K} , \mathbf{C}_2 , \mathbf{C}_1 stands for the time at t_{n+1} . The initial value of the predictor of $\dot{\mathbf{d}}_1$ at the time t_{n+1} is

$$(\dot{\mathbf{d}}_1^{n+1})_{i=0}^p = \dot{\mathbf{d}}_1(\mathbf{x}_n, t_n) = \mathbf{T} \dot{\mathbf{d}}_1(\mathbf{x}_{n+1}, t_n) + \dot{\bar{\mathbf{R}}}_f(\mathbf{x}_{n+1}, t_n) \quad (76)$$

Equation (74) is non-linear and an iterative procedure for its solution is now necessary. The recurrence relations can be established by inserting the value of $\Delta \dot{\mathbf{d}}_1$ at each iteration into equations (61), (62), (71) and (69) to update the predictor values of \mathbf{c}_m , \mathbf{d}_1 .

It is of interest to remark that the computation of the matrix \mathbf{T} is related to the generalized convective velocity field $\dot{\mathbf{U}}_w^*$ and the time interval Δt . Generally Δt for the integration in time

domain can be taken as constant, so that the matrix \mathbf{T} is computed for a problem only once in the case of steady state flow ($\dot{\mathbf{U}}_{\mathbf{w}}^*$ is constant). For an unsteady state flow problem, the matrix \mathbf{T} has to be computed at each time step. This will require more computational efforts and is unacceptable for practice even though the time step size by using the present method can be considerably increased with high accuracy as compared with the explicit characteristic Galerkin approach and other implicit algorithm such as SUPG (the Stream Upwind Petrov Galerkin) method. To consider the variation of $\dot{\mathbf{U}}_{\mathbf{w}}^*$ with time we may split the unsteady state velocity field into the two parts, i.e. the constant one $\dot{\mathbf{U}}_{\mathbf{w}0}^*$ and the variation $\Delta\dot{\mathbf{U}}_{\mathbf{w}}^*(t)$ on $\dot{\mathbf{U}}_{\mathbf{w}0}^*$

$$\dot{\mathbf{U}}_{\mathbf{w}}^*(t) = \dot{\mathbf{U}}_{\mathbf{w}0}^* + \Delta\dot{\mathbf{U}}_{\mathbf{w}}^*(t) \quad (77)$$

Then equation (42) can be written as

$$\dot{\mathbf{d}}_1^* = (\mathbf{H}_0 + \Delta\mathbf{H}_1(t))\mathbf{d}_1^* + \bar{\mathbf{r}}_f \quad (78)$$

where

$$\begin{aligned} \mathbf{H}_0 &= -\mathbf{M}^{-1}\mathbf{C}_{1,11}^0, \quad \mathbf{C}_1^0 = \int_{\Omega} \mathbf{N} \dot{\mathbf{U}}_{\mathbf{w}0,j}^* \frac{\partial \mathbf{N}^T}{\partial x_j} d\Omega \\ \Delta\mathbf{H}_1(t) &= -\mathbf{M}^{-1}\mathbf{C}_{1,11}^t, \quad \mathbf{C}_1^t(t) = \int_{\Omega} \mathbf{N} \Delta\dot{\mathbf{U}}_{\mathbf{w},j}^*(t) \frac{\partial \mathbf{N}^T}{\partial x_j} d\Omega \end{aligned} \quad (79)$$

Similar to integration of equation (42), integration of equation (78) in the time interval $\Delta t = [t_n, t_{n+1}]$ gives the solution

$$\mathbf{d}_1^*(\mathbf{x}_{n+1}, t_{n+1}) = \mathbf{T}\mathbf{d}_1^*(\mathbf{x}_{n+1}, t_n) + \bar{\mathbf{R}}_f = \mathbf{T}\mathbf{d}_1(\mathbf{x}_{n+1}, t_n) + \bar{\mathbf{R}}_f \quad (80)$$

with

$$\mathbf{T} = \exp(\mathbf{H}^*\Delta t) = \exp((\mathbf{H}_0 + \Delta\mathbf{H}_1)\Delta t) = \mathbf{T}_0(\Delta\mathbf{T}) \quad (81)$$

$$\mathbf{T}_0 = \exp(\mathbf{H}_0 \Delta t) \quad (82)$$

$$\Delta\mathbf{T} = \exp(\Delta\mathbf{H}_1 \Delta t) \quad (83)$$

The exponential matrix \mathbf{T}_0 is still computed by using the 2^N algorithm described in equations (47)–(50). As it is assumed that $\|\Delta\dot{\mathbf{U}}_{\mathbf{w}}^*(t)\| \ll \|\dot{\mathbf{U}}_{\mathbf{w}0}^*\|$, the exponential matrix $\Delta\mathbf{T}$ can be calculated with first-order approximation and without using the precise integration scheme, i.e.

$$\Delta\mathbf{T} = \exp(\Delta\mathbf{H}_1 \Delta t) \approx \mathbf{I} + \Delta\mathbf{H}_1 \Delta t \quad (84)$$

Then the exponential matrix \mathbf{T}_0 is calculated only once or a limited number of times for unsteady state flow problems. For the latter case, the exponential matrix \mathbf{T}_0 will be updated when it is needed for ensuring the accuracy of the exponential matrix \mathbf{T} .

4. STABILITY ANALYSIS

To fulfil stability analysis of the present algorithm in time domain, we consider the time discretization for the semi-discretized finite element equation of the governing equation (53) in the

homogeneous form, which gives

$$\mathbf{M}(\phi^{n+1} - \mathbf{T}\phi^n) + (\mathbf{K} + \mathbf{C}_2)(\gamma\phi^{n+1} + (1 - \gamma)\mathbf{T}\phi^n)\Delta t = 0 \quad (85)$$

Re-arranging equation (85) we have

$$[\mathbf{I} + \gamma \Delta t \mathbf{M}^{-1}(\mathbf{K} + \mathbf{C}_2)]\phi^{n+1} = [\mathbf{I} - (1 - \gamma)\Delta t \mathbf{M}^{-1}(\mathbf{K} + \mathbf{C}_2)]\mathbf{T}\phi^n \quad (86)$$

With modal decomposition approach,²⁴ equation (86) can be decomposed into uncoupled scalar equations as

$$[1 + \gamma \Delta t(\lambda_k + \lambda_c)]\phi^{n+1} = [1 - (1 - \gamma)\Delta t(\lambda_k + \lambda_c)]T\phi^n \quad (87)$$

Noting that $[1 + \gamma \Delta t(\lambda_k + \lambda_c)] > 0$ for all allowable values of the parameters due to the property of the matrices \mathbf{M} , \mathbf{K} , \mathbf{C}_2 , we re-write equation (87) as

$$\phi^{n+1} = \lambda\phi^n \quad (88)$$

where $\lambda = [1 - (1 - \gamma)\Delta t(\lambda_k + \lambda_c)]T/[1 + \gamma \Delta t(\lambda_k + \lambda_c)]$ is the amplification factor. The stability requirement can be expressed as

$$-1 < \frac{[1 - (1 - \gamma)\Delta t(\lambda_k + \lambda_c)]T}{1 + \gamma \Delta t(\lambda_k + \lambda_c)} < 1. \quad (89)$$

It is noted that $\|\mathbf{H} \Delta t\| \leq 0$ according to the definitions of matrices \mathbf{H} , \mathbf{C}_1 , \mathbf{M} in equations (43), consequently, we have $0 \leq T \leq 1$ in equation (89). Hence, the right-hand inequality of equation (89) is satisfied for all allowable values of parameters, and the left-hand inequality is satisfied whenever $\gamma \geq T/(1 + T)$, which is equal to or less than $1/2$.

5. NUMERICAL RESULTS

As the first example, a one dimensional problem¹³ is considered. A soil column is 30 m long and 1 m high. It is meshed by 30×1 uniform four noded isoparametric elements. A Gaussian concentration distribution of unit initial amplitude centred at co-ordinate $x = 5.0$ m, shown in Figure 1, is applied. The steady and uniform intrinsic velocity field with $\bar{U}_{w,x} \equiv 1$ m/s over the column is assumed. In the first case, only the transport of pollutants by pure advective flow, i.e. with the infinite value of Peclet number, is involved. It is noted that the value of the critical time step size for the present pure advective problem, required by the stability condition of the explicit algorithm is $\Delta t_{cr} = \sqrt{1/3}$ s,¹⁷ which corresponds to the value $C_{r,crit} = \sqrt{1/3}$. As we use the present implicit characteristic Galerkin method to solve for this test case, a series of values of the Courant number, ranging from $\Delta t = 2$ s to $\Delta t = 20$ s (i.e. from $C_r = 2$ to $C_r = 20$), is taken. It is remarked that the identical results are obtained for all the cases using different values of the Courant number as shown in Figure 1, while SUPG fails to run the test case with $C_r \geq 2$. In addition, it is observed that the results obtained by using the present implicit characteristic Galerkin method agree very well with the exact solutions and perform better than those given by the explicit characteristic Galerkin method¹⁴ and SUPG method.^{12,25} The reason for the identical results obtained by using the present method with the use of different values of Courant number is due to the precise integration procedure, which entirely determines the accuracy of the solution of the purely convective problem. Indeed there is no Newmark-like numerical integration in time domain involved in the solution procedure for this test case. It is also shown that no

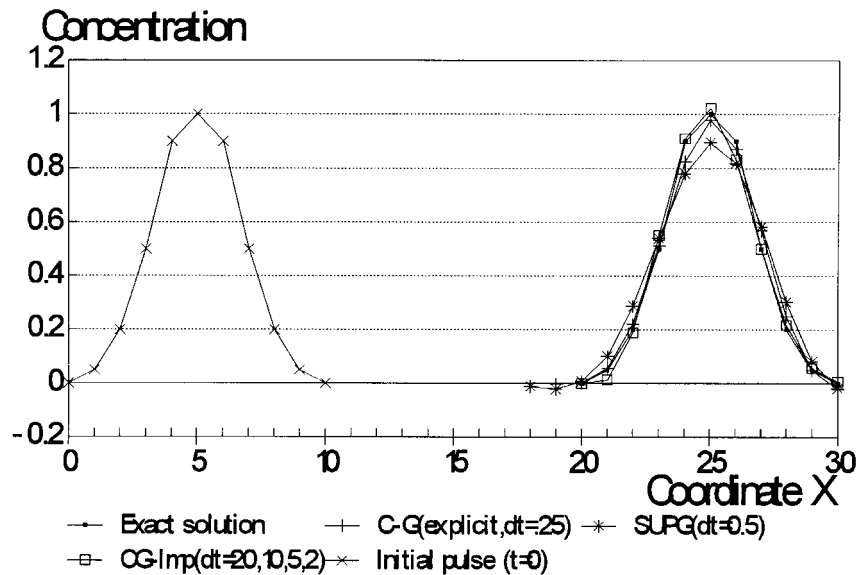


Figure 1. Concentration distribution at $t = 20$ s for a purely convection case

numerical decay of the amplitude of the Gaussian concentration distribution appears in the present procedure as the concentration distribution moves along the axis of the column with time, while the numerical decay can be obviously observed for SUPG in Figure 1.

From the case 2 to the case 4 of the first example, we consider the pollutant transport with the same initial concentration distribution and velocity field, but governed by different mechanisms. The second case considers the transport process governed by advection, dispersion and immobile water effect phenomena, in which the following parameters are used, i.e. $a_L = 0.1$ m, mass transfer coefficient from the fluid in motion to the immobile water $\alpha_d^* = 8.0448 \times 10^{-3} \text{ s}^{-1}$, the portion of the immobile water $S_{w0} = 0.25$ in saturation degree of water $S_w = 0.5$. A comparison of the concentration distribution curves at time $t = 14$ s obtained by using different values of $C_r = 0.25, 0.5, 1.0, 2.0$ is illustrated in Figure 2. A comparison of the results given by the implicit and the explicit characteristic Galerkin scheme is also illustrated in Figure 2. The third case is to demonstrate the capability of the proposed model to model the contaminant transport through unsaturated soils when all the governing phenomena, including both physical and chemical non-equilibrium processes, are present. In addition to the parameters used in the second case of the example, the data to describe the remaining governing mechanisms are as follows: equilibrium sorption with the distribution coefficient $K_d = 0.01 \text{ m}^3/\text{kg}$ and the portion of the fluid-solid contact surface $p = 0.5$ which concerns immobile water, linear degradation with degradation coefficients $k_s = 0.5 \text{ s}^{-1}$, $k_m = k_{im} = 0.01 \text{ s}^{-1}$, and non-equilibrium sorption with the sorption rate $K_1 = 5.3466E - 3 \text{ m}^3/\text{kg s}$, the desorption rate $K_2 = 6.2234E - 5 \text{ s}^{-1}$ and the maximum of the non-equilibrium sorbed solute $F_0 = 1.0$. Figure 3 presents a comparison of the results of concentration distribution at time $t = 10$ s as $C_r = 0.25, 0.5, 1.0, 2.0$ are used. Figures 2 and 3 illustrate good performance of the present method in unconditional stability as the value of Courant number increases and convergence as the value of Courant number decreases. The errors

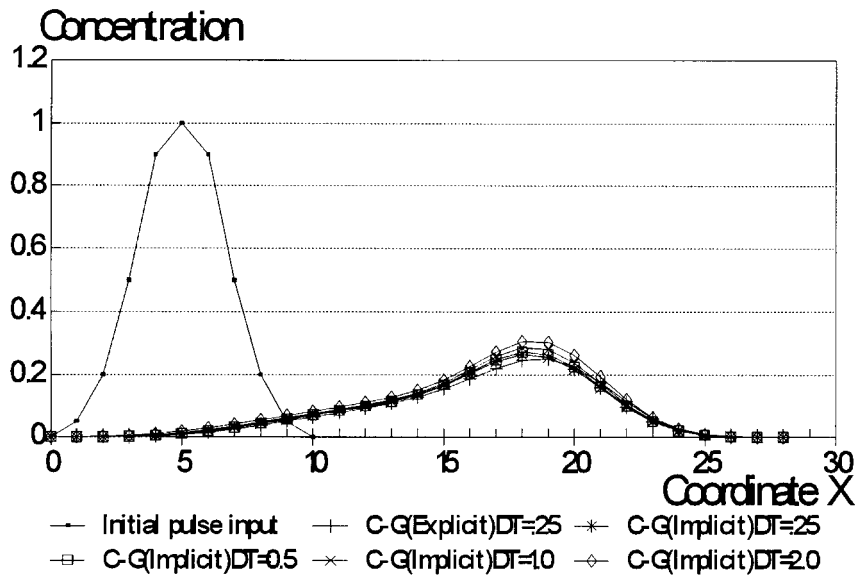


Figure 2. Concentration distribution at $t = 14$ s for advection-dispersion-immobile water effect case

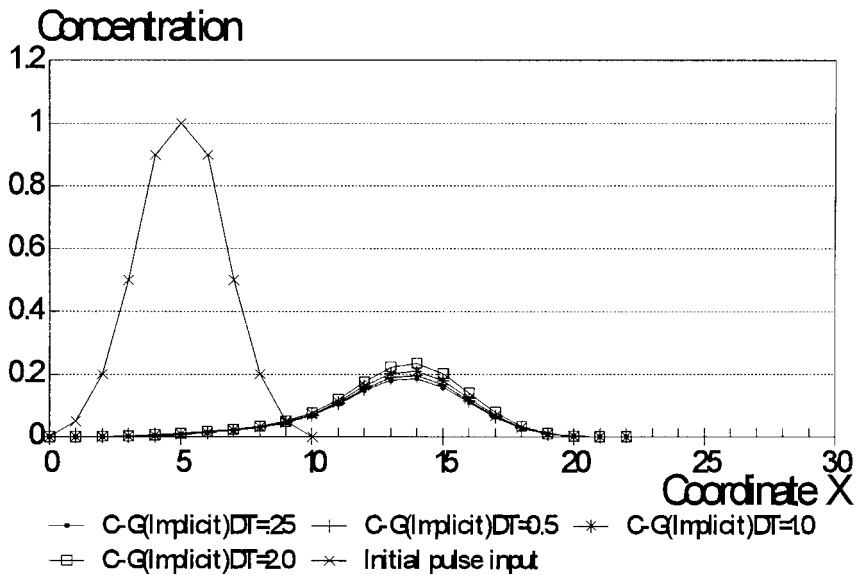


Figure 3. Concentration distribution at $t = 10$ s for advection-dispersion-sorption-immobile water effect, degradation case

in concentration values at the peaks of the curves can be explained by a relatively large value of Courant number used, and by the transport and sorption related-non-equilibrium processes involved. Nevertheless, the errors decrease with reduced values of Courant number.

To illustrate the effects of various mechanisms on the pollutant transport, we consider the fourth case of the example. The contaminant transport in this case is governed by four sub test cases, respectively, as follows: (1) The same test case as that presented in the third case above, i.e. all the governing phenomena, including both physical (transport related) and chemical (sorption related) non-equilibrium processes, are present; the parameters used are also the same as those used in the third case; (2) the same test case as above but without the physical non-equilibrium; (3) the same test case as for sub-case (1) but without chemical non-equilibrium; (4) the same test case as for sub-case (1) but without both non-equilibrium processes. Figure 4 gives a comparison of the concentration distribution at time $t = 10$ s for the four sub-test cases when $C_r = 2.0$ is used.

As a second example, in order to validate the performance of the present numerical model for cases including more mechanisms governing pollutant transport in unsaturated soils and boundary condition different from that in the first numerical example, we analyse the solute transport in an aqueous solution with Na^+ and Cd^{2+} in a soil sample column since experimental results for the example with Na^+ are available¹⁵ and numerical results obtained by using the present model can be compared with the experimental results. The example considers a soil sample column with 7.9 cm high, porosity $n = 0.32$ and $\rho_s = 2.57$. In the experiment, the top of the sample is open to the air and the bottom is open to the vacuum tank. The pressure at the bottom can be controlled so as to maintain a pressure difference between the two ends of the sample. Fluid (water or the solution) inflow is injected from the top of the sample and its flux rate is controlled by a fluid supply system. In the experimental procedure, both the pressure difference ΔP and the rate of the inflow flux \dot{w} are kept constant as the particular values $\Delta P = 2 \text{ kpa}$ and $\dot{w} = 1.3557 \text{ cm/h}$ are used, so that the porous water flow as well as the distribution of saturation degree of water in the

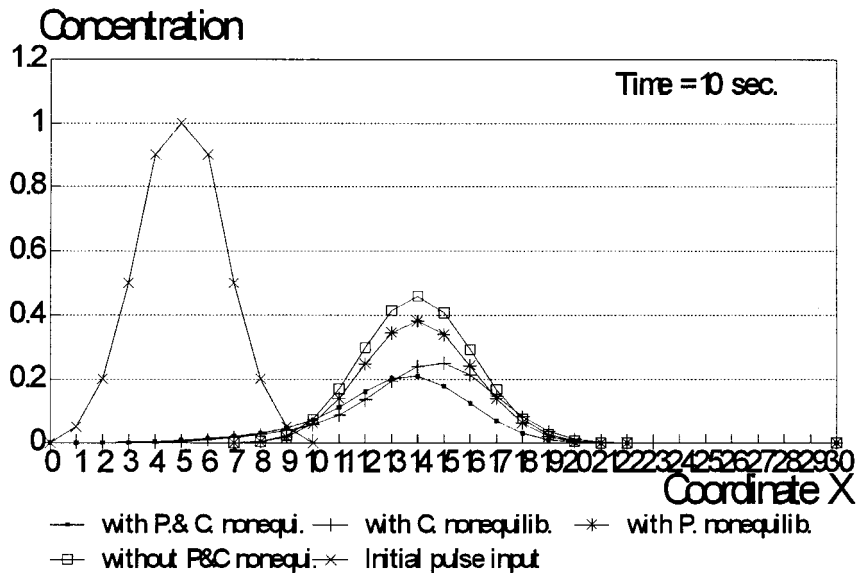


Figure 4. Concentration distribution at $t = 10$ s for advection-dispersion-sorption-immobile water effect, degradation case: with and without physical and/or chemical non-equilibrium processes

sample approach a steady state. In addition, the measured saturation degrees of water over the sample are approximately uniform with an average value $S_w = 0.65125$ and a deviation value of about one per cent from the average value. Then, the injected water flux is polluted with the normalized unit concentration of Na^+ . The contaminant transport is assumedly governed by convection and hydrodynamic dispersion with $a_L = 0.672 \text{ cm}$ and equilibrium sorption with $K_d = 0.1741 \text{ cm}^3/\text{g}$. To carry out the finite element analysis, the sample is meshed by 50×1 uniform four noded elements. Figure 5 gives a comparison between numerical and experimental results of the concentration in outflow from the column bottom at a series of time instants. It is illustrated that the numerical results obtained by using $C_r = 20.586, 10.293, 5.147, 2.573$ agree well with the measured experimental results. It should be remarked that in the experimental study, the values of the concentration in outflow from the column bottom are measured and the material parameters a_L and K_d are determined by an inverse analysis method (the Gradient-Regularization method¹⁵). Therefore, the experimental results are taken rather as a reference solution instead of an exact (real) solution of the problem.

The second case of this example considers the transport of metal Cadmium Cd^{2+} miscible in the injected water with the normalized unit concentration. It is assumed that the contaminant transport process is governed by convection, hydrodynamic dispersion with $a_L = 0.3738 \text{ cm}$, equilibrium sorption with $K_d = 0.1013 \text{ cm}^3/\text{g}$ and non-equilibrium sorption with $K_1 = 5.3466E - 4 \text{ m}^3/\text{kg s}$, $K_2 = 6.2234E - 6 \text{ s}^{-1}$, $F_0 = 1.0$. It is noted that the extreme solute value F_0 of Cd^{2+} sorbed to the solid skeleton of the soil sample is also normalized here, similar to the normalization for the value of the concentration of Cd^{2+} injected into the soil sample with water inflow. Figure 6 illustrates the concentrations of Cd^{2+} in outflow from the bottom of the soil sample at a series of time instant when $C_r = 20.586, 10.293, 5.147, 2.573$ are taken.

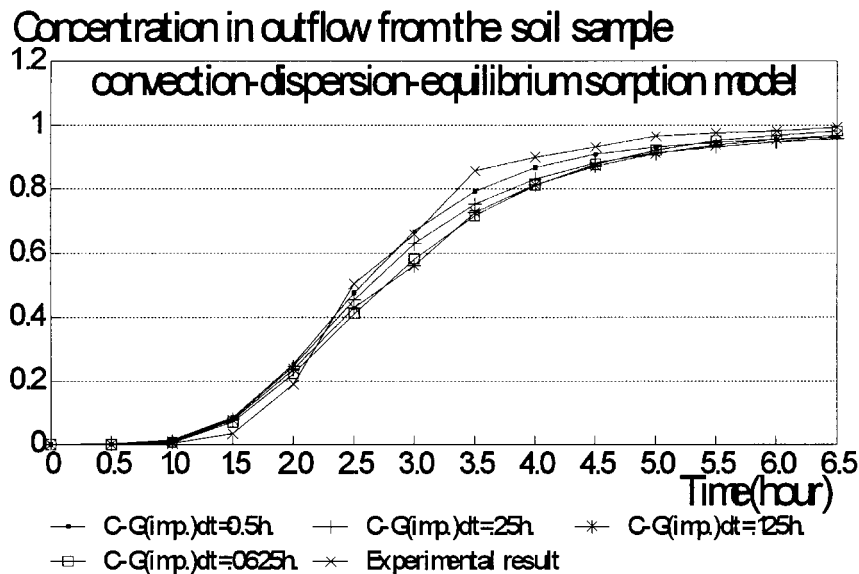


Figure 5. Comparison between numerical and experimental results for pollutant transport of Nitrates

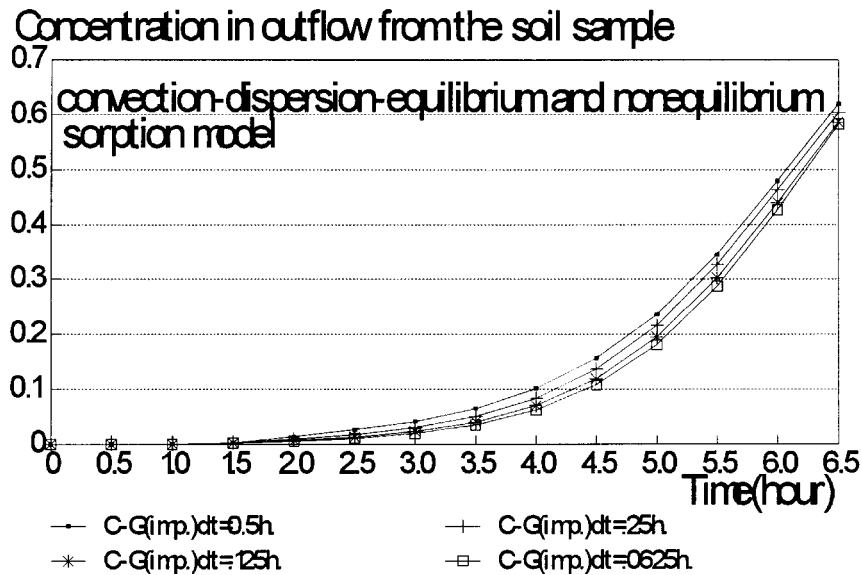


Figure 6. Concentration of metal Cadmium in outflow from the soil sample at a series of time instants.

The third example is a 2D problem taken from Brooks and Hughes.²⁵ The initial and the boundary conditions of the example were also depicted by Radu *et al.*¹³ As the transient solution for the example can be regarded as a device to obtain the steady-state solution, the performance on this example becomes a reference criterion to validate the proposed method. The domain is a 10×10 m square and a 10×10 square mesh in space is used. The constant concentration with unity value is imposed along the bottom boundary edge and the lower 3 m of the left boundary edge, while the concentration at the remaining part of the boundary is specified as zero. The convective velocity has a value $\|\vec{U}_w\| = 1$ m/s and is oriented with an angle of $\vartheta = 60^\circ$ with respect to the bottom boundary edge. Two test cases are considered. The governing mechanisms and the parameters used in the two cases are: (1) convection and dispersion with $a_L = a_T = 0.6$ m. (2) convection, dispersion with $a_L = a_T = 0.5$ m., equilibrium linear sorption with $K_d = 0.01$ m³/kg and $p = 0.5$, linear degradation with $k_s = k_m = k_{im} = 0.01$ s⁻¹, immobile water effect with $\alpha_d^* = 8.0448 \times 10^{-3}$ s⁻¹, $S_{w0} = 0.25$ in $S_{w0} = 0.5$, and non-equilibrium sorption with $K_1 = 5.3466E - 2$ m³/kg s, $K_2 = 6.2234E - 4$ s⁻¹, $F_0 = 1.0$.

Figure 7 illustrate the concentration contours at steady states for the case 1 as $C_r = 0.866$, 1.732, 3.467 and 6.933 are used. Figures 7(a) and 7(b) illustrate that the concentration distributions obtained by using $C_r = 0.866$ and 1.732 for the case 1 are almost identical, while it was reported²⁶ that for the same example with $\vartheta = 60^\circ$ serious spatial oscillations appear and the solution is highly deteriorated if C_r is larger than one for the SUPG approach. In addition, the solutions, as shown in Figures 7(c) and 7(d) respectively, provided by the present approach are still stable as larger values of Courant number, i.e. $C_r = 3.467$ and 6.933, are used, even though with certain amount of numerical error (but it seems acceptable).

Figure 8 gives the concentration contours at steady states for the case 2 as $C_r = 0.866$, 1.732 are used. The purpose of the test cases 2 in this example is to show the capability of the present

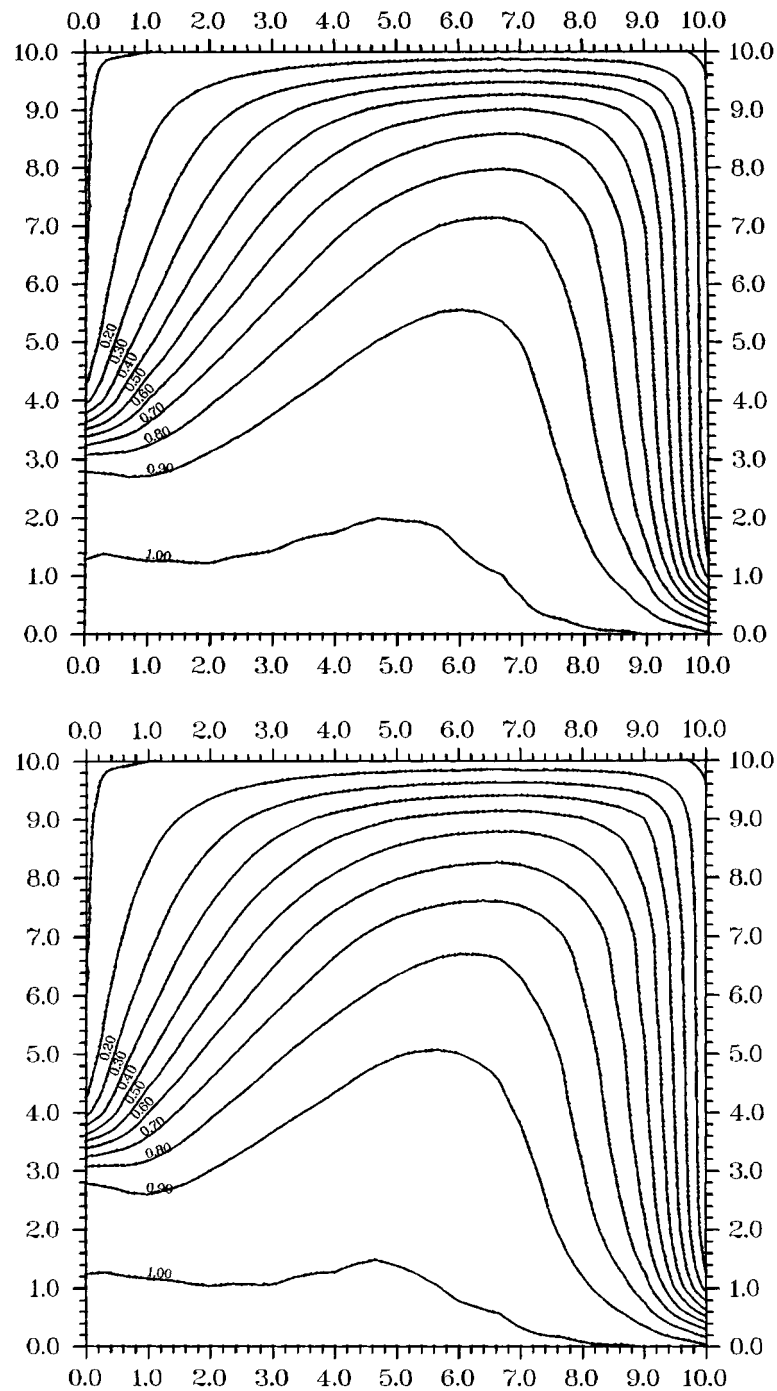


Figure 7. Concentration contours of Hughes's problem: advection-dispersion case ($P_e = 2.31$, $\theta = 60^\circ$) ((a) $C_r = 0.866$; (b) $C_r = 1.732$; (c) $C_r = 3.467$; (d) $C_r = 6.933$)

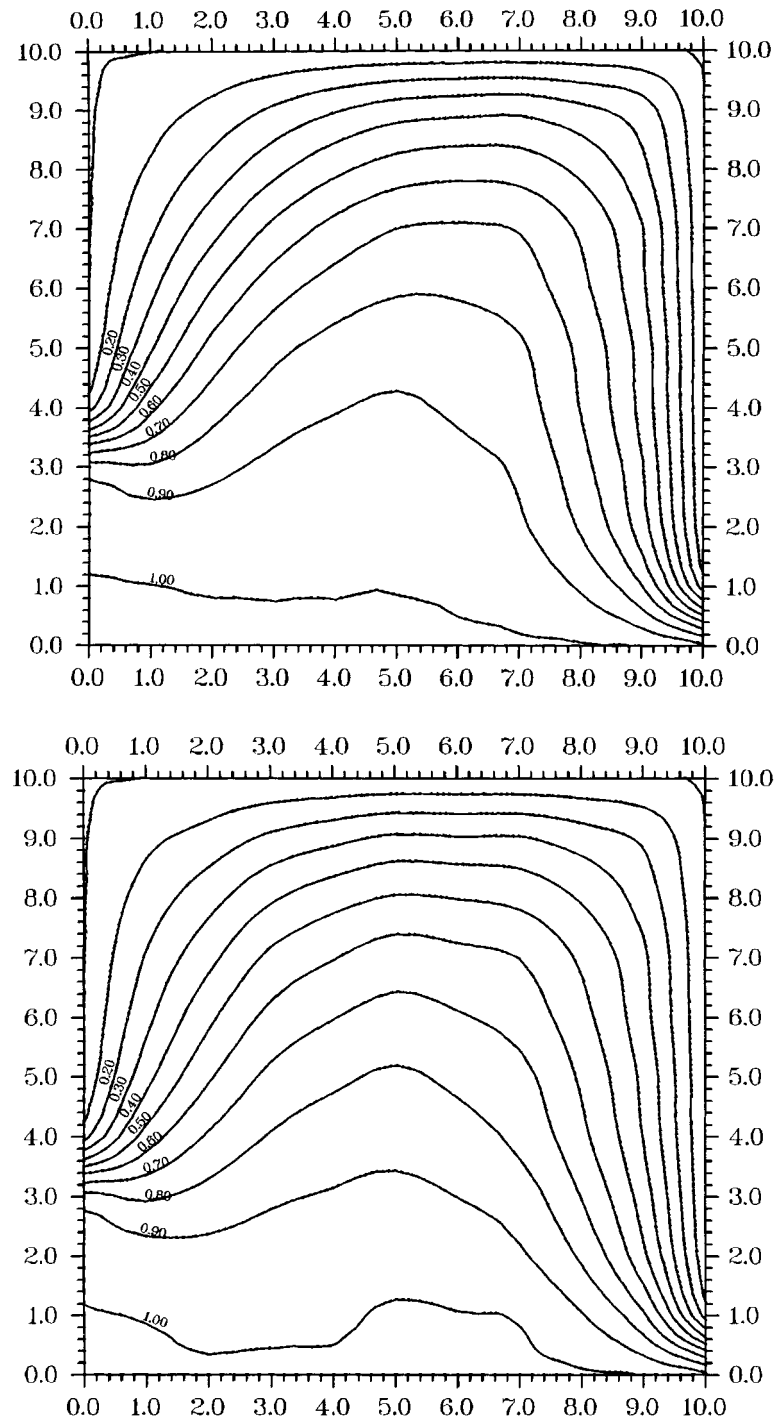


Figure 7. Continued.

approach to model the pollutant transport in two-dimensional domain, in which all the phenomena governing the contaminant transport are present; in addition, to show the unconditional stability and the accuracy of the numerical solution procedure.

6. CONCLUSION

This paper presents a numerical model for predicting contaminant transport in unsaturated soils. The purpose of the model is to simultaneously simulate the six physical and chemical phenomena, including both physical and chemical non-equilibrium processes, governing miscible contaminant transport in unsaturated-saturated soils. A finite element procedure, based on the characteristic Galerkin method with an implicit algorithm and a precise integration procedure, is developed to numerically solve the model equations. The key point of the present approach is that the spatial co-ordinate is convected along the problem characteristics. Then convective terms disappear and the remaining problem becomes self-adjoint and can be discretized by using the standard Galerkin procedure in space domain. The logical basis of the characteristic Galerkin approach provides the optimal procedure for the advection-diffusion problems with scalar variables. In addition, based on the operator splitting procedure, the precise integration procedure is introduced to determine the material derivative and the physical quantities at material points in the governing equation of the problem. Then an implicit algorithm with a combination of both the precise and the traditional numerical integration procedures, for the characteristic

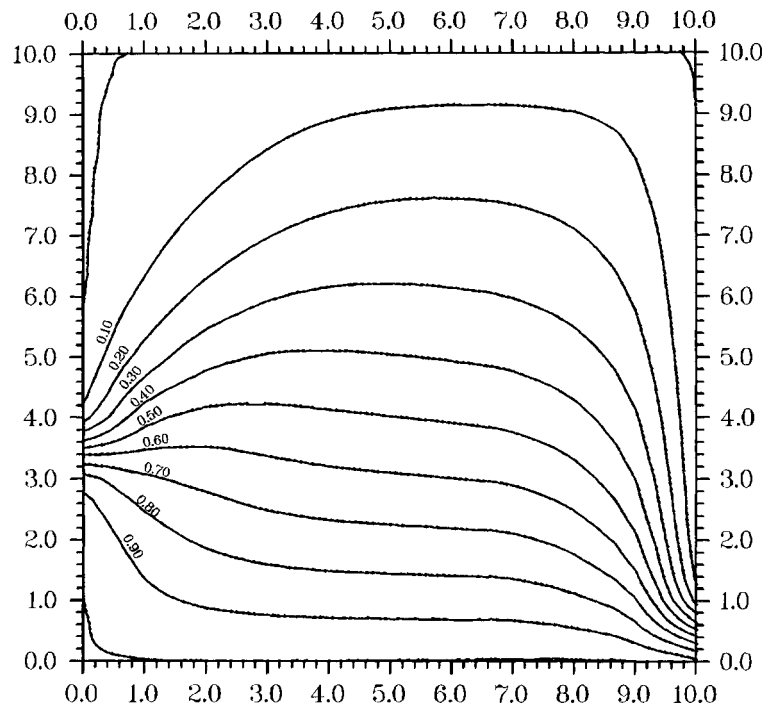


Figure 8. Concentration contours of Hughes's problem: advection-dispersion-equilibrium linear sorption-immobile water effect-linear degradation, nonequilibrium sorption case ($\theta = 60^\circ$; (a) $C_r = 0.866$; (b) $C_r = 3.467$)

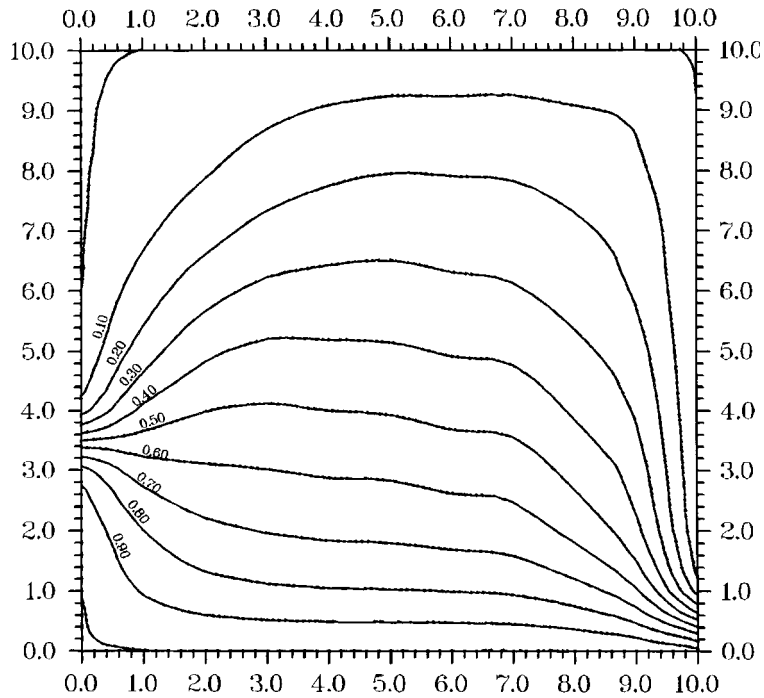


Figure 8. Continued.

Galerkin method is formulated. The stability analysis shows that the unconditional stability of present algorithm is enhanced as compared with that of the traditional implicit numerical integration procedure. It is remarked that the present algorithm can also be applied to numerically solve a variety of initial and boundary value problems representing a typical convection–diffusion process with a scalar-dependent variable.

ACKNOWLEDGEMENTS

This work is sponsored by the European Commission Research Project CI1*CT94-0014 and the National Natural Science Foundation of China. The support is greatly acknowledged.

REFERENCES

1. J. Bear and A. Verruijt, *Modelling Groundwater Flow and Pollution*, D. Reidel, Dordrecht, Netherlands, 1987.
2. R. N. Yong, A. M. O. Mohamed and B.P. Warkentin, *Principles of Contaminant Transport in Soils*, Elsevier, Netherlands, 1992.
3. M. L. Brusseau, R. E. Jessup and P. S. C. Rao, 'Modeling the transport of solutes influenced by multiprocess non-equilibrium', *Water Resour. Res.*, **25**, 1971–1988 (1989).
4. H. Kandil, C. T. Miller and R. W. Skaggs, 'Modelling long-term solute transport in drained unsaturated zones', *Water Resour. Res.*, **28**, 2799–2809 (1992).
5. D. W. Smith, R. K. Rowe and J. P. Booker, 'The analysis of pollutant migration through soil with linear hereditary time-dependent sorption', *Int. J. Numer. Anal. Meth. Geomech.*, **17**, 255–274 (1993).

6. B. A. Schrefler, F. E. in environmental engineering: coupled thermo-hydro-mechanical processes in porous media including pollutant transport, *Arch. Comput. Meth. Engng.*, **2**(3), 1–54 (1995).
7. R. N. Yong, H. R. Thomas (eds), *Proc. Geoenvironmental Engineering Conf.*, Cardiff, U.K., 16–18 September 1997.
8. R. W. Lewis and B. A. Schrefler, *The Finite Element Method in the Deformation and Consolidation of Porous Media*, Wiley, Chichester, 1987.
9. Xikui Li, O. C. Zienkiewicz and Y. M. Xie, 'A numerical model for immiscible two-phase fluid flow in a porous medium and its time domain solution', *Int. J. Numer. Meth. Engng.*, **30**, 1195–1212 (1990).
10. B. A. Schrefler, L. Simoni, Xikui Li and O. C. Zienkiewicz, Mechanics of partially saturated porous media, in C. S. Desai and G. Gioda (eds), *Numerical Method and Constitutive Modelling in Geomechanics*, CISM Courses and Lectures, Springer Berlin, 1990, pp. 169–210.
11. Xikui Li, H. R. Thomas and Yiqun Fan, Finite element method and constitutive modelling and computation for unsaturated soils, *Comput. Meth. Appl. Mech. Engng.*, **169**, 135–159 (1999).
12. P. Biver, Modelling transport in a double porosity medium: an alternative approach, *Proc. Int. Conf. of Water Pollution: Modelling Measuring and Prediction*, Southampton, U.K., Computational Mechanics Publications, Elsevier Science, Amsterdam, 1991, pp. 45–57.
13. J. P. Radu, P. Biver, R. Charlier and S. Cescotto, '2D and 3D finite element modelling of miscible pollutant transport in groundwater, below the unsaturated zone', *Proc. Int. Conf. of Hydrodynamics, ICHD'94*, 30 October–3 November 1994, Wuxi, China.
14. Xikui Li, J. Radu and R. Charlier, 'Numerical modelling of miscible pollutant transport by groundwater in unsaturated zones', *Proc. 9th Int. Conf. for Computer Methods and Advances in Geomechanics*, Wuhan, China, 1997, pp. 1255–1260.
15. Baoyuan Li, Zhaohui Zhu, Aixiang Zhang, Hongho Zheng, Suling Liu, Liangru Jiang and Weixian Mu, 'The experimental study on the transport of Na^+ and Cd^{++} in unsaturated soil', *Proc. 2nd Int. Conf. on Unsaturated Soils*, Int. Academic Publishers, Beijing, China, 1998.
16. O. C. Zienkiewicz and R. L. Taylor, *The Finite Element Methods*, Chapter 12, 4th edn., Vol. 2, McGraw-Hill, U.K., 1991.
17. O. C. Zienkiewicz and R. Codina, 'A general algorithm for compressible and incompressible flow—Part I. The split, characteristic-based scheme', *Int. J. Numer. Meth. Fluids*, **20**, 869–885 (1995).
18. T. J. R. Hughes, 'Recent progress in the development and understanding of S. U. P. G. methods with special reference to the compressible Euler and Navier-Stokes equations', *Int. J. Numer. Meth. Fluids*, **7**, 1261–1275 (1987).
19. R. Codina, 'Stability analysis of the forward Euler scheme for the convection-diffusion equation using SUPG formulation in space', *Int. J. Numer. Meth. Engng.*, **36**, 1445–1464 (1993).
20. A. J. Chorin, 'A numerical method for solving incompressible viscous problems', *J. Comput. Phys.*, **2**, 12–26 (1967).
21. Wanxie Zhong, Jianping Zhu and Xiangxiang Zhong, 'A precise time integration algorithm for nonlinear system', *Proc. 3rd WCCM*, Tezuka Microfilm Co. Ltd., Tokyo, 1994, pp. 12–17.
22. E. Angel and R. Bellman, *Dynamic Programming and Partial Differential Equations*, Academic Press, New York, 1972.
23. Zhaochang Liu, Lansheng Zhang, Yongfeng Nie and Kun Zhu, *Control of Pollutants in Underground Water System*, Environmental Science Publishers of China, Beijing, China, 1991 (in Chinese).
24. T. J. R. Hughes, *The Finite Element Method*, Prentice-Hall, Englewood Cliffs, NJ, 1987.
25. A. N. Brooks and T. J. R. Hughes, 'Streamline upwind Petrov Galerkin formulation for convection dominated flows with particular emphasis on the incompressible Navier-Stokes equation', *Comput. Meth. Appl. Mech. Engng.*, **32**, 199–259 (1982).
26. J. P. Radu, *Annual Report for EC Project*, University of Liege, Belgium, 1997.
27. O. C. Zienkiewicz and R. L. Taylor, *The Finite Element Methods*, 4th edn., Vol. 1, McGraw-Hill, U.K., 1989.